

## TIME REVERSAL ACOUSTICS

M. FINK, G. MONTALDO and M TANTER.

Laboratoire Ondes et Acoustique, ESPCI, Université Paris VII,  
U.M.R. C.N.R.S. 7587, 10 rue Vauquelin, 75005 Paris, France.

### 1. Introduction

Since more than ten years, time reversal techniques have been developed in many different fields of applications including detection of defects in solids, underwater acoustics, room acoustics but also ultrasound medical imaging and therapy. The essential property that makes time reversed acoustics possible is that the underlying physical process of wave propagation would be unchanged if time were reversed. In a non dissipative medium, the equations governing the waves guarantee that for every burst of sound that diverges from a source there exists in theory a set of waves that would precisely retrace the path of the sound back to the source. This remains true even if the propagation medium is inhomogeneous and presents variations of density and compressibility which reflect, scatter and refract the sound. If the source is pointlike, this allows focusing back on the source whatever the medium complexity. . For this reason, time reversal represents a very powerful adaptive focusing technique for complex media. The generation of this reconverging wave can be achieved by using the so called Time Reversal Mirrors (T.R.M). It is made of arrays of reversible piezoelectric transducers that can record the wavefield coming from the sources and send back its time-reversed version in the medium. It relies on the use of fully programmable multi-channels electronics. Each transducer has its own electronics : amplifier, analog-digital converter, digital memories and a programmable generator capable of synthesizing the temporal inverted signal stored in the memory.

In the first section of this paper, we will focus on the ability of using passive reflecting targets embedded in the body (kidney stones, breast microcalcifications....) as sources of time reversal waves. Real time tracking and destruction of moving kidney stones will be demonstrated in the case of lithotripsy application. We will show the strong potential of iterative time reversal techniques in multiple targets environments to select and focus in real time on each target of a medium. The ability of iterative time reversal to improve the detection of microcalcifications in a random scattering media (speckle noise) will be also presented. We will show that distorsions induced by sound velocity heterogeneities are compensated by the iterative time reversal technique guaranteeing the maximum pressure to be reached at the target position.

In the second section of this paper, we will discuss the time reversal focusing properties observed in dissipative media like skull. We will show that the time reversal focal spot can be strongly degraded as, in such medium, we can no more rely on the time reversal invariance of the wave equation. Important sidelobes appear around the main focus. However, combining time reversal with amplitude compensation techniques allows correction of absorption effects and decreasing of these sidelobes. Application of this coupled technique to high precision brain hyperthermia through the skull will be demonstrated.

Beyond these straightforward applications of time reversal to spatial focusing of waves through aberrating medium, we will show that time reversal techniques allow also to revisit the complete concept of piezoelectric transducer designing. Contrary to conventional transducer technology avoiding unwanted reverberations in piezoelectric elements, time reversal can take benefit of strongly reverberating media to increase the transducer efficiency. We will demonstrate that very high pressure fields (1000 Atm.) can be obtained with a few number of transducers connected to reverberating media such as solid waveguides. The dispersive property of waveguides is compensated by time reversal allowing very long coded excitations to be recompressed in very short high amplitude pulses. It leads to a new generation of ultra-compact shock wave lithotripters that used a very small transducer number.

## **2. The time-reversal mirror in pulse echo mode.**

One of the most promising area for the application of TRMs is pulse-echo detection. In this domain, one is interested in detection, imaging and sometimes destruction of passive reflecting targets. A set of transducers first sends a short impulse and then detects the various echoes from the targets. One looks for calcifications, kidney or gallbladder stones, tumors. As the acoustic detection quality depends on the availability of the sharpest possible ultrasonic beams to scan the medium of interest, the presence of an aberrating medium between the targets and the transducers can drastically change both the beam profiles and the detection capability. In medical imaging, a fat layer of varying thickness, bone tissues, or some muscular tissues may greatly degrade focusing.

For such applications, a TRM array can be controlled according to a three-steps sequence (Fig.1.). One part of the array generates a brief pulse to illuminate the region of interest through any aberrating medium. If the region contains a point-like reflector, the reflected wavefront is selected by means of a temporal window and then the acquired information is time-reversed and reemitted. The reemitted wavefront refocuses on the target through the medium. It compensates also for unknown deformation of the mirror array. Although this self-focusing technique is highly effective, it requires the presence of a reflecting target in the medium [1].

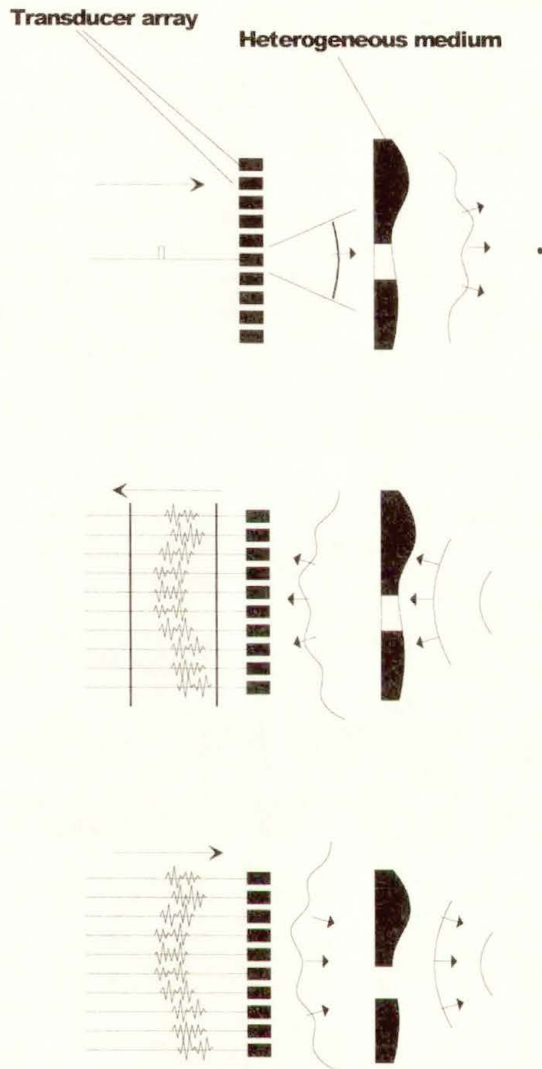


Fig.1. TRM focusing through inhomogeneous media requires three steps. The first step (1a) consists in transmitting a wavefront through the inhomogeneous medium from the array to the target. The target generates a backscattered pressure field that propagates through the inhomogeneous medium and is distorted. The second step is the recording step (1b); the backscattered pressure field is recorded by the transducer array. In the last step (1c) the transducer array generates on its surface the time reversed field. This pressure field propagates through the aberrating medium, and focuses on the target.

### 2.1. Selective focusing through an inhomogeneous medium with the iterative time-reversal process.

In media containing several targets, the problem is more complicated and iterations of the TR operation may be used to select one target. Indeed, if the medium contains two targets of different reflectivities, the time-reversal of the echoes reflected from these targets generates two wavefronts focused on each target. The mirror produces the real acoustic images of the two reflectors on themselves. The highest amplitude wavefront illuminates the most reflective target, while the weakest wavefront illuminates the second target. In this case, the time-reversal process can be iterated. After the first time-reversed illumination, the weakest target is illuminated more weakly and reflects a fainter wavefront than the one coming from the strongest target. After some iterations, the process converges and produces a wavefront focused on the most reflective target. It converges if the target separation is sufficient to avoid the illumination of one target by the real acoustic image of the other one [2].

Experiments have been performed with a linear array of 128 elements working at central frequency 3.5 MHz. They demonstrate the ability of TRM iterative mode to select the most reflective target in a multiple target medium. For example, An aberrating layer was placed between the array and a medium made of two different wires (0.2 mm and 0.4 mm diameter copper wires) situated at a depth  $z = 90$  mm from the array (Fig.2.).

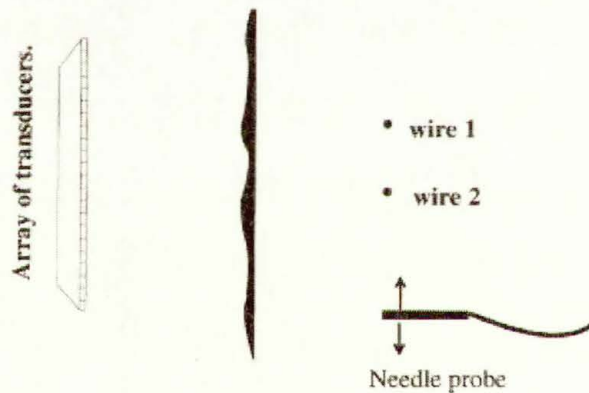


Fig. 2. Experimental set-up.

In the first step, one transducer of the array illuminates an angular sector containing the two wires. After the first illumination, the echoes from the two targets are recorded. Fig. 3a shows the recorded data corresponding to the two individual wave fronts pointing at the two wires. The recorded signals are then time-reversed and retransmitted. The time-reversed waves propagated and the new directivity pattern is measured by scanning the plane  $z = 90$  mm with the hydrophone.

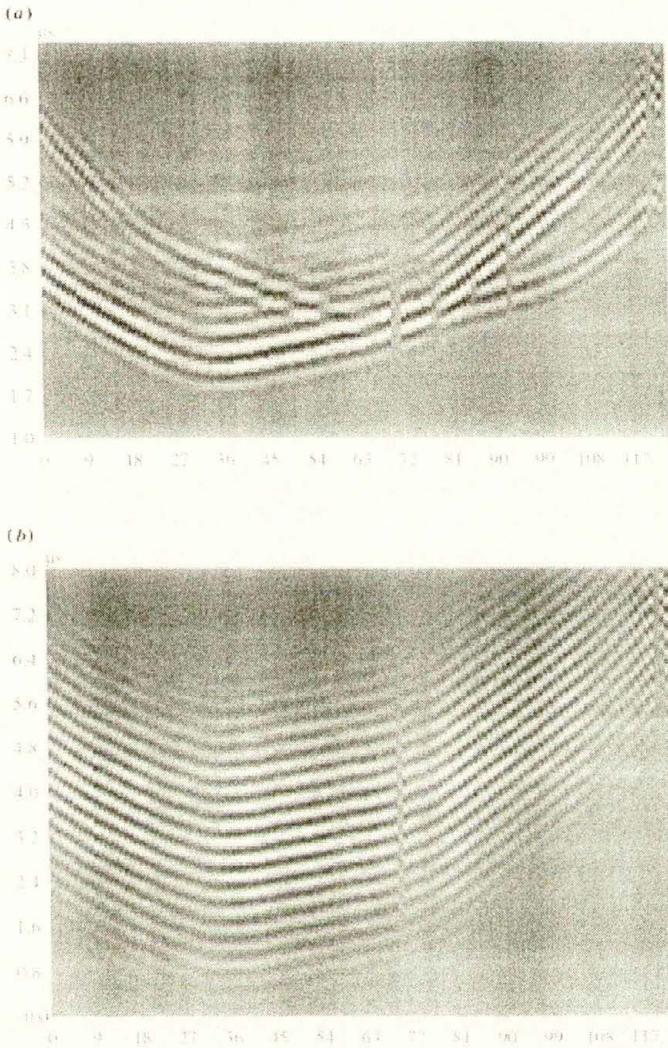


Fig. 3. (a) Echographic signals observed from the two wires after the first illumination. (b) Echographic signals observed after four iterations of the time reversal process.

The solid line of Fig.4. represents the directivity pattern which shows two maxima corresponding to the two target locations. The pressure field reaches a higher value at the location of the wire whose scattering cross section is larger. The process is iterated : the new echoes from the wires were recorded, time-reversed and retransmitted, etc. As the process is iterated, the wire which reflects less energy receives a weaker time-reversed wave. This is shown on Fig. 4 which corresponds to the directivity pattern of the first to the fourth iteration.

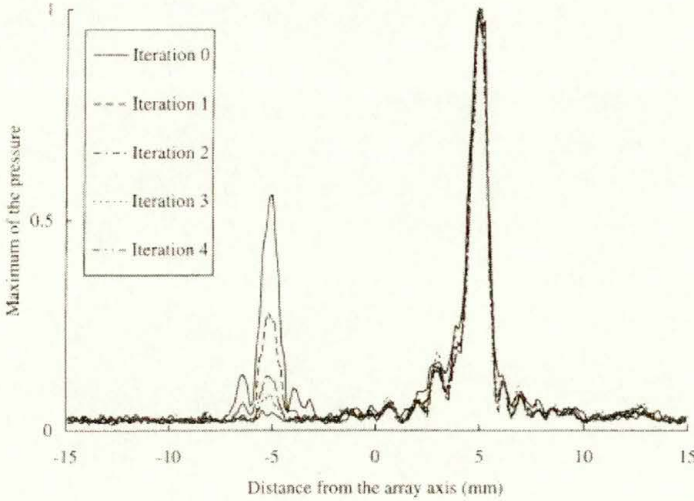


Fig.4. Directivity patterns measured in the wire plane after each iteration.

The small wire is no more illuminated after the last emission. Fig. 3b represents the reflected wavefronts recorded by the array after the fourth iteration (note that the wavefront has a longer duration because of the multiple iterations, that imply a repeated effect of the acousto-electric transducer response).

Such experiments demonstrate the ability of TRM iterative mode to select the most reflective target in a multiple target medium. This may be interpreted as a learning process that selects among several wave fronts the one coming from the most important reflector.

## 2.2. Application to lithotripsy

The method of choice to treat kidney and gall stones involves the use of large amplitude acoustic shock waves that are generated extracorporeally and focused onto a stone within the body. Lithotripters typically have a high focusing gain so that pressures are high at the stone but substantially lower in the surrounding tissue. The alignment of stone in the patient with the lithotripter focus is accomplished with fluoroscopy or ultrasonic imaging. Focusing is achieved geometrically, i.e., with ellipsoidal reflectors, concave focusing arrays of piezoelectric transducers, or acoustic lenses. Shock waves have amplitudes at the focus on the order of 1000 bar and a duration of a few microseconds. They are typically fired at a 1 s pulse repetition rate [3,4]. The main problem to overcome in the field of lithotripsy is related to stone motion due to breathing. Indeed, the lateral dimension of the shock wave in current lithotripsy devices is less than 5 mm and the amplitude of the stone displacement can reach up to 20 mm from the initial position. Hence, In classical focusing technique shock waves often miss the stone and submit neighboring tissues to unnecessary shocks that may cause local bleeding.

Different approaches have been investigated to overcome these limitations. Most of them are based on a trigger of the high power pulses when the stone goes through

the focus of the shock wave generator. These approaches may reduce the number of shots needed to disintegrate the stone but increase considerably the time of treatment. The use of 2D arrays of piezoelectric transducers has opened the possibility of electronic steering and focusing the beam in biological tissues and a time-reversal piezoelectric generator has been developed [5] to electronically move the focus and track the stone during a lithotripsy treatment. The goal is to locate and focus on a given reflecting target among others, as for example, a stone in its surrounding: others stones and organ walls. Moreover, the stone is not a point like reflector but has dimensions up to ten times the wavelength. In the basic procedure that has been developed, the region of interest is first insonified by the transducer array. The reflected field is sensed on the whole array, time-reversed and retransmitted. As the process is iterated, the ultrasonic beam selects the target with the highest reflectivity. If the target is spatially extended, the process converges on one spot, whose dimensions depend only on geometry of the time-reversal mirror and the wavelength. High amplification during the last iteration can be used to produce a shock wave for stone destruction. However, two problems limit this technique. For human applications, it is necessary to use very short high power signals (bipolar and unipolar pulses) to prevent damages caused in the organs by cavitation gas bubbles, while the iterated pulses have long duration. Besides, a complete time-reversal electronic is expensive and the number of time-reversal channels must be limited. To solve these problems, another procedure has been developed. In the first step, only a subgroup of the array is used in a time-reversed mode. This step is conducted with low power ultrasound in order to remain in linear acoustics. After some iterations, a low power ultrasonic beam, generated by the array subgroup, is focused on the stone. The last set of received signals are used to deduce a time of flight profile on the subgroup. This time of flight profile is then interpolated to the whole array. The final step consists in the generation, by the whole array, of very short high power signals with the correct delays.

Time-reversal experiments are performed with bidimensional transducer arrays working at a central frequency of 360 kHz, especially designed for lithotripsy. They are made of 121 prefocused piezo-composite transducer elements arranged on a spherical cup of 190 mm radius of curvature (see fig. 5). To illustrate the efficiency of the time-reversal approach, two focusing experiments are presented in the following. The first one is conducted on a gallbladder stone of approximately spherical shape. The other one deals with a large kidney stone of irregular shape.

In the gallbladder experiment, the stone has a diameter of 18 mm, much larger than the ultrasound wavelength of 4 mm. The stone is at a depth  $z=170$  mm from the surface of the array and at position  $x=10$  mm,  $y=20$  mm off-axis.

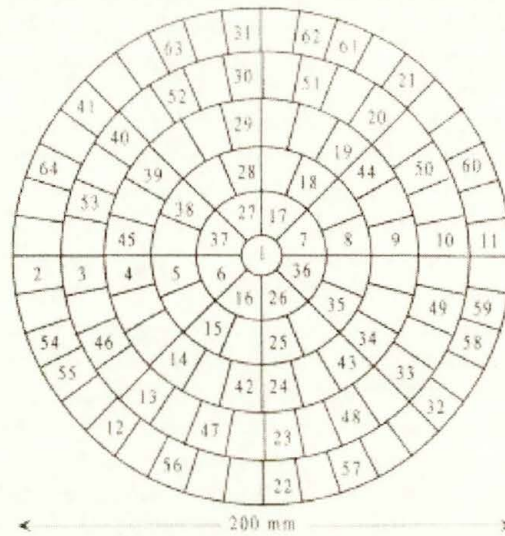


Fig. 5. Geometry of the prefocused two dimensional time-reversal mirror developed for lithotripsy. The connected elements are numbered.

In the first step, a pulse is transmitted by a single transducer element located in the center of the array. The echoes from the stone are recorded by a subgroup of 64 transducers (Fig. 6). Each line is normalized in the display and the 64 signals are presented from channel 1 to channel 64. On each channel, the first echo comes from the specular reflection on the surface of the stone. These signals have the same temporal shape. They line up according to a wavefront characterizing the location of the stone. Approximately  $10 \mu\text{s}$  after this signal, a second echo is observed on several channels corresponding to a creeping wave or to a secondary diffraction on the back side of the stone.

In the second step, the stone is removed and the recorded signals are time-reversed and retransmitted. The time-reversed wave propagates and the resulting pressure pattern is measured with an hydrophone in the plane of the stone ( Fig. 7). The pressure field is focused on a bright point of the stone. Indeed, the  $-6 \text{ dB}$  beam width is equal to  $5.9 \text{ mm}$ , which is the dimension of the array point spread function at this location whereas the stone diameter is about  $18 \text{ mm}$ . Thus, the time-reversal process has focused the beam on a spot whose dimensions depend only on the geometry of the array and the location of the stone.

In order to explain such a focusing on a small portion of an extended target, we take into account only the specular echoes whose amplitudes are much higher than those resulting from the elastic response. From the scattering point of view, the target shell may be considered as a continuous set of target points of different scattering strengths. The first backscattered wavefront results from the interference pattern of the wavelets scattered by each elementary surface element of the stone.

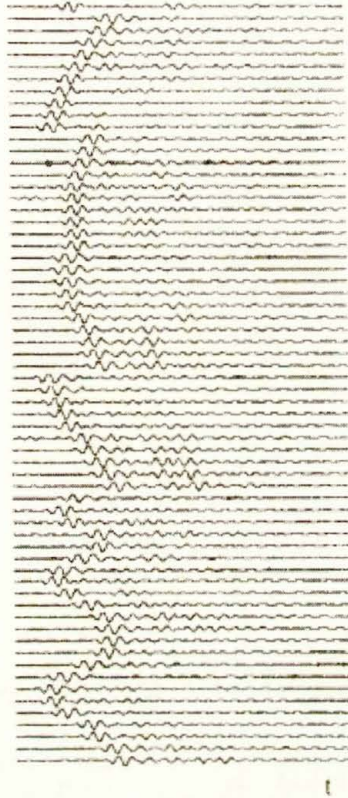


Fig. 6. Echographic signals recorded from a gall-bladder stone after the first illumination.

One of these surface elements yields a significant echo only if the wavelets scattered in its region interfere constructively on the surface of the transducer array. Such a bright point is located on a surface element for which the acoustic path is extremum (stationary phase theorem).

The stone has a spherical shape and a surface roughness which is very small compared to the ultrasound wavelength (4 mm). In the case of a first illumination with a single element, there is only one bright point for each receiving element. Moreover, a simple geometric analysis shows that all these bright points are located on a surface of dimensions equivalent to a disk of diameter 5 mm. Thus, the wavefront backscattered by this stone comes from a small region whose dimension is about one wavelength. This experiment shows, that even in the case of an extended target, the time-reversal process selects the brightest point of its surface and the resulting beam focuses on a spot with dimensions of the order of the diffraction point spread function.

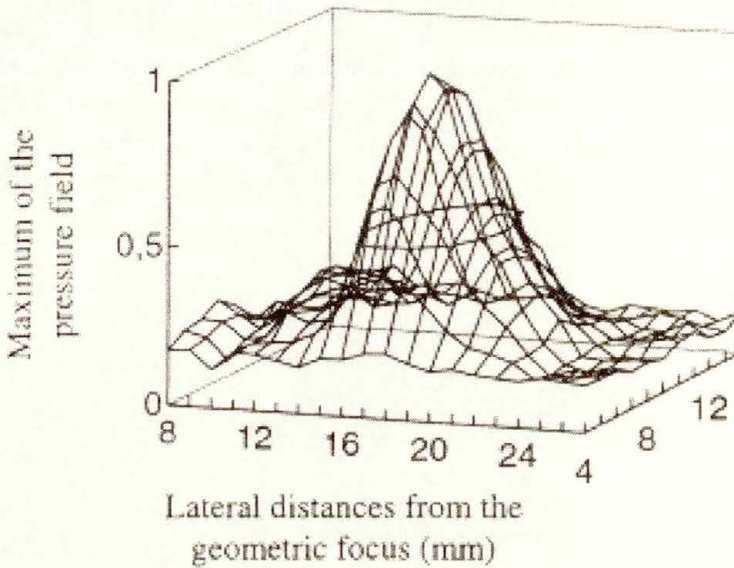


Fig. 7. Directivity pattern (maximum of the pressure field) measured in the plane of the gall bladder stone,  $z=170$  mm. The 64 transducers transmit simultaneously the time reversed signals of figure 6.

The second experiment is performed with a kidney stone of large dimensions (approximately  $x=30$  mm,  $y=20$  mm and  $z=20$  mm). This stone is much larger than the previous one and its shape has irregularities of the size of the wavelength. It has several bright points and iteration of the time-reversal process is needed to obtain a sharp focusing. The stone is located near the geometrical focus and a pulse is transmitted by a single element located at the center of the array. After the first illumination, echoes from the stone are recorded by the 64 connected transducers (Fig. 8a). We observe that the shape of the signal can be very different from one transducer to the other. There are several bright points on the surface of the stone and the waves reflected by them interfere in the plane that contains the array. Moreover, elastic responses are higher than in the previous experiment.

At this step, the time-reversal process is iterated and the corresponding wavefronts recorded. Fig. 9 shows the directivity patterns along an axis parallel to both the array aperture and the greatest dimension of the stone. The directivity pattern corresponding to the first iteration confirms that the wave sensed on the array comes from several bright points. There is one main lobe (whose dimensions correspond to the diffraction point spread function) and two side lobes. On the next iteration, the side lobes level decreases significantly, but after four iterations, it remains relatively high. These bright points have a similar echogenicity and hence many iterations are required to select the brightest one.

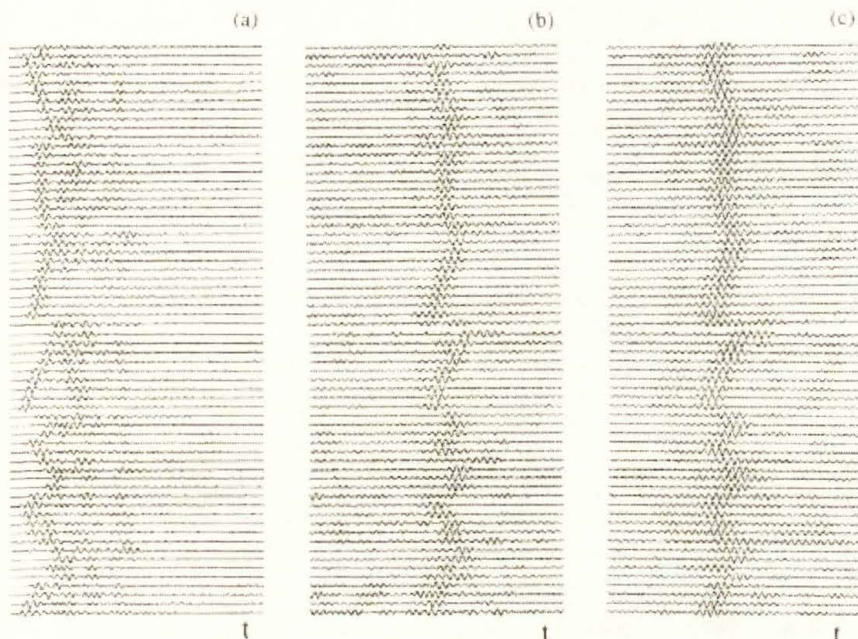


Fig. 8. Echographic signals recorded from a kidney stone after the initial illumination (a), the second (b) and the fifth (c) iteration of the time-reversal process.

A numerical method has been implemented both to optimize the side lobe level in homogeneous propagating medium and to use very short high power signals in order to prevent cavitation. First, the time of flight between the bright point selected by the iterative time-reversal process and each transducer is determined. A classical mean to determine the arrival time of echoes from a point-like reflector is to use cross-correlation between signals from neighboring transducer elements. However, for a complex target like a stone, the spatial coherence of the backscattered wave can be very limited. Indeed, as seen in the previous experiment, specular echoes from an extended target may result from the interference of wavelets coming from several bright points and thus be very different from one element to the other. Moreover depending on the transducer element, one or two replicas of the specular echo can be observed (Fig. 8a). The accuracy with which these arrival times can be estimated is then limited by the degree of correlation between received signals. The iterative time-reversal process is a spatial filter which selects the brightest surface element and hence, improve the level of coherence across the array (Fig. 8c). Nevertheless, the calculation of the relative times of flight between signals using the cross-correlation technique is time consuming. The time-reversal process achieves an analogical correlation of the interelement impulse response and so, the offsets of the peak in the signals measured after a time-reversal operation gives a much faster determination of the arrival times.

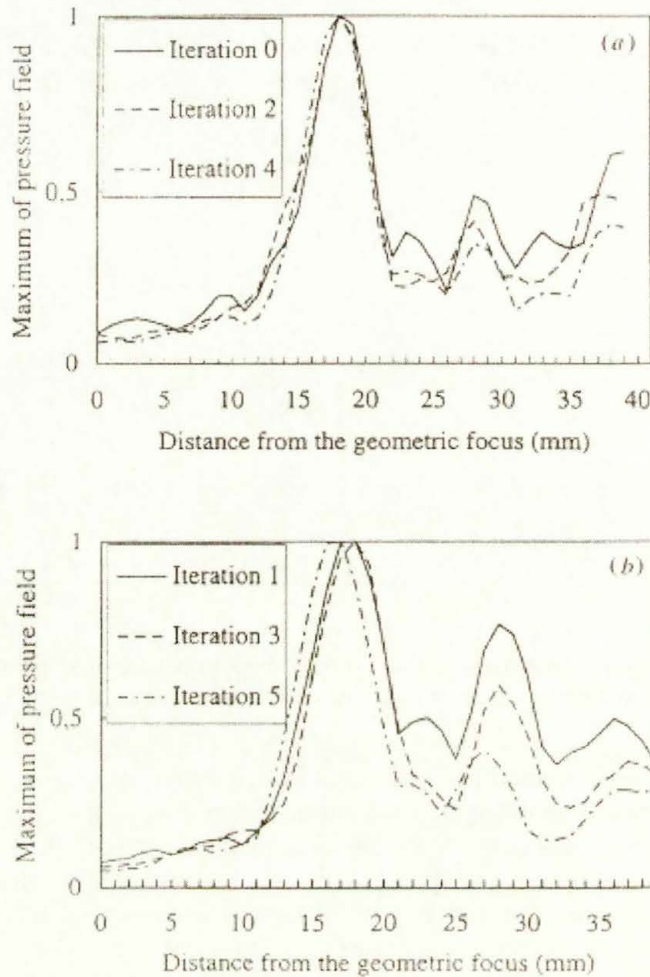


Fig. 9. Directivity patterns along the y axis at iterations 0, 2, 4 (a) and iterations 1, 3, 5 (b).

Finally, this set of experimental time delays is fitted to a model, that depends on the unknown spatial coordinates,  $x, y, z$ , of the bright point. The medium of propagation is assumed to be homogeneous (distortions due to refraction in tissues is very weak at 360 kHz). The estimated coordinates are used to steer a very short beam. The focusing obtained on the one hand with the iterative time-reversal process and on the other hand with time shifted pulses (according to the estimated coordinates) can now be compared (Fig.10). Both acoustic beams focus at the same location and that the algorithm improves spatial filtering: The main lobe is sharper and the secondary lobe has been eliminated. Moreover, the time delay profile can be now interpolated to the 121 transducers, which allows the generation of the high power ultrasound beam from the whole array. Another advantage of this optimization method is to provide controls on the process. First, the tracking area can be limited and the shock wave triggered only if the estimated location of

the stone is in the region defined by the physician. Second, the quality of the match between the time shifting law and a spherical model provides a way to assess whether the echoes come from one bright point.

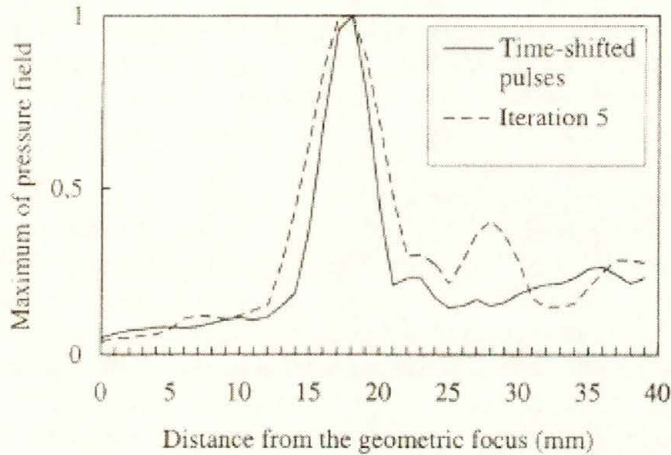


Fig. 10. Comparison of the directivity patterns along the y axis obtained with the time-reversal process and pulses time-shifted according to the estimated co-ordinates.

A prototype especially designed for TRM experiments in the field of lithotripsy has been developed. It is able to calculate the coordinates of one bright point of the target in less than 40 ms and in a region of 60 mm along the axis and 40 mm laterally. Many in-vitro and in vivo experiments with kidney or gall bladder stones have shown the efficiency of the method. However, this system is quite expensive and we will show in paragraph 3 that new approaches minimizing the transducer number have recently been developed.

### 2.3 Multiple target detection

Iterative time reversal technique is well adapted to focus on the target of higher reflectivity. However, in many cases it is also interesting to learn how to focus on the other reflectors. In order to achieve selective detection and focusing on each reflector inside an unknown multitarget medium, a matrix formalism approach, that extended time reversal analysis, was developed by Prada et al [6,7,8]. This method is derived from the theoretical analysis of iterative TRM and consists in the construction of the invariant of the time reversal process. This analysis consists in determining the possible transmitted waveforms that are invariant under the time reversal process. For these waveforms an iteration of the time reversal operation gives stationary results. Such waveforms can be determined through the calculation of the eigenvectors of the so called time reversal operator. Indeed, the echoes of a single target are an eigenvector of the time reversal operator  $K^*K$ , where  $K=K(\omega)$  represents the inter-element response matrix.

Using this basic idea that each target is associated to an eigenvector of the time reversal operator, it is possible to record the whole time reversal operator and compute its eigenvectors decomposition. Thanks to this numerical eigenvectors decomposition, a selective focusing on each target can be achieved. Using this technique, known as the DORT method, Chambers et al. recently shown that the spectrum of the time reversal operator can be complex and very informative [9].

Nevertheless, the D.O.R.T method suffers several limitations as it requires the measurement of the  $N \times N$  inter-element impulse responses and the computation of the eigenvectors decomposition is quite time consuming and do not allow real time imaging.

A new real time technique has been recently proposed by G.Montaldo et al [10] for multitarget selective focusing that does not require the experimental acquisition of the time reversal operator. Actually, this technique achieves the operator decomposition simply by using a particular sequence of iterative waves illuminations instead of computational power. The general idea of this new approach is first to use the time reversal iterative process in order to estimate the signals focusing on the brightest target. These signals are then used to derive a cancellation filter allowing to cancel this target echoes during the selection of the next brightest spot by iterative time reversal. This process can be extended to following multiple targets detection using the cancellation filter that cleans up the targets already detected. The drawback of temporal spreading induced during the iterative time reversal selection is also overcome by introducing a "pulse compression operator". This filter uses the narrowband signals deduced from the iteration to reconstruct a set of wideband pulsed signals focusing on the selected target. This set of pulsed signals focusing on a given target corresponds to a spatio-temporal eigenvector of the time reversal operator and so is called "eigenpulse". Using such eigenpulses allows to achieve a lot of iterations without expanding the signal duration. In order to explain the iterative decomposition method, a simple homogeneous medium containing only 3 diffusers is considered. The experiments are conducted in the ultrasonic range in a water tank. The acoustic waves are emitted and received with a standard linear array made of 120 elements working at a 1.5 MHz central frequency. The process learns to identify each target step by step beginning from the most reflective one to the weakest one. The selective identification of a new target is made in three steps.

1. A plane wave is first emitted in this medium. The backscattered signals are composed of three wavefronts of different amplitudes corresponding to each target (Fig. 11.a). If these signals are time reversed and reemitted through the medium, the resulting wavefronts focus on each target and the brightest target is more illuminated than the others. Consequently, its contribution in the backscattered echoes is more important. After a few iterations this time-reversal process permits to select the most reflecting reflector. However, at each iteration the signals are filtered by the limited bandwidth of the transducers and it results in a progressive temporal spreading of the emission signals. In figure 11b we can see the received signal after 8 iterations of the time-reversal process, the

strongest scatterer was selected but the bandwidth was clearly reduced. The second step of the process allows to overcome this problem.

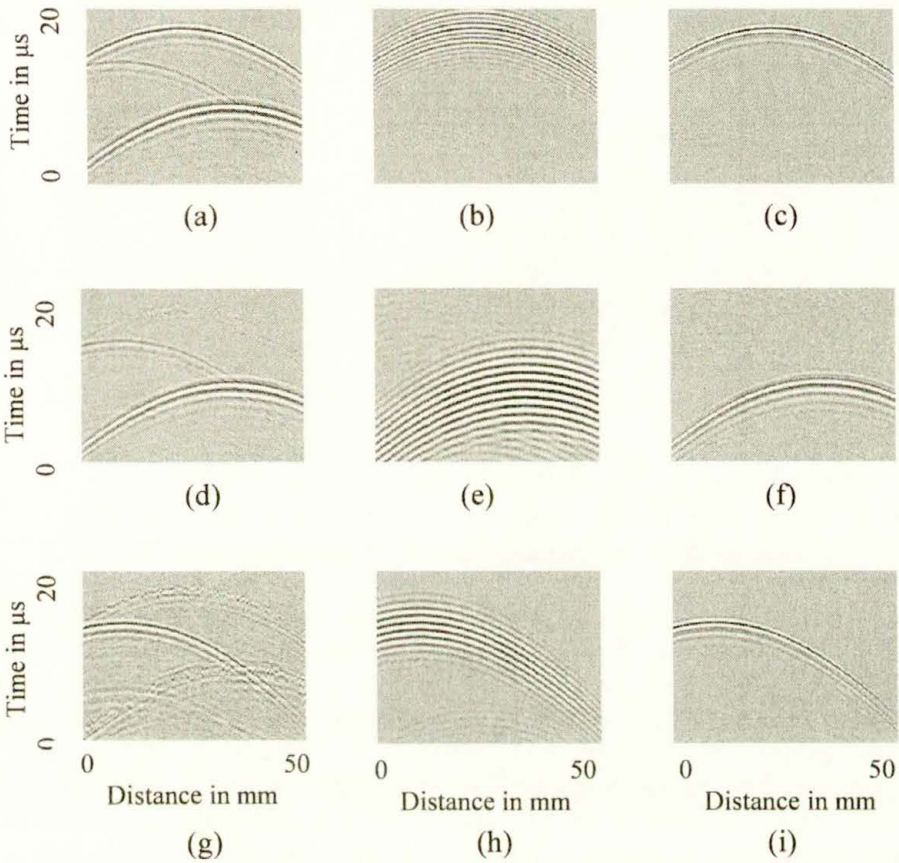


Fig. 11. The iterative process.

- (a) Backscattered echoes of the 3 reflectors after a plane wave emission.
- (b) Detection of the strongest reflector by iterative time reversal.
- (c) "Eigenpulse" of the stronger reflector.
- (d) Backscattered echoes of the two reflectors after filtering the first one.
- (e) Detection of the second reflector by time reversal and filtering.
- (f) "Eigenpulse" of the second reflector.
- (g) Signal of the 3rd reflector after filtering the first and second.
- (h) Detection of the 3rd reflector by time reversal and filtering.
- (i) Eigenpulse of the 3rd reflector.

2. The bandwidth narrowing suffered during the time reversal process is a real drawback in most applications. An easy solution consists to reconstruct a wideband wavefront at each iteration by detecting the arrival time and amplitude

law of the signals received on each transducer. These arrival time and amplitude law is then used to reemit a wideband pulsed signal identical on each transducer with the corresponding amplitudes and time delays on each transducers. It allows to avoid the bandwidth spreading of the signals during the iterative process. The arrival time and amplitude can be measured by using a simple maximum detection technique for each transducer (see Fig. 12).

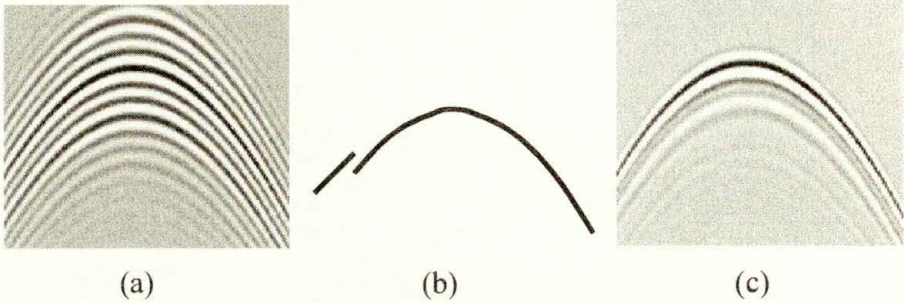


Fig. 12.

- (a) After iterating the time reversal process, the signal is spread in time.
- (b) During the maximum detection process,  $2\pi$  phase errors can occur.
- (c) After emitting this wavefront, we obtain a backscattered narrow pulse,  $2\pi$  phase errors do not appear during the identification of the wavefront.

Such a "pulsed" wavefront construction before each time reversal emission allows to correct the temporal spreading of the signals during the iterative process (see Fig. 12.c and 11.c). In general, the use of a simple algorithm for the "pulsed wavefront" construction (for example a maximum detection) can induce some errors in the arrival time estimation. For example, if the signal is composed of several sinusoids as presented in fig. 12.a, the maximum detection can be limited by a  $2\pi$  uncertainty (fig. 12 b). It results in the reemission of an incorrect wavefront at the next illumination. However, most part of the energy of this incorrect wavefront is focused on the good location and the maximum detection on the next backscattered echoes becomes easier and more accurate. Thus, a few iterations of the time reversal process combined with the pulse compression allow to obtain a correct pulsed wave front or "eigenpulse" signal. Note that the duration of these combined steps is only limited by the waves travel time and the maximum detection hardware. As an example, for medical applications, the detection of a brightest target located at 50 mm depth in tissues achieved in 8 iterations of these combined steps could last less than a millisecond.

3. The basic idea for selecting a new reflector is to filter the signals coming from the detected ones. This filter is built by subtracting the projection of the wave front from the signal each time. If we start with a backscattered signal containing the echoes of the three reflectors (Fig. 11.a), we obtain the filtered signals shown in Fig. 11.d. As one can notice, the echoes of the strongest reflector have been cancelled. This new set of filtered signals is now used as

initial illumination for the iterative time reversal process. The cancellation filter is applied at each step during the iterative time reversal process. Consequently, the second target generates the brightest echoes and is progressively selected by the iteration process (Fig. 11.e). The signals backscattered by the second target are temporally spread and can be “pulse compressed” (Fig. 11.f). Finally, the cancellation filter allows to cancel the first and second target and select the third target by iterating the time reversal process. Figures 11.g, 11.h and 11.i, describe the final eigenvector decomposition that was found for the third and weakest target.

As one can notice, the complete process does not require any fastidious calculation. The combination of a simple maximum detection with the iterative time reversal process was found sufficient in order to select multiple targets. The cancellation filter corresponds also to a simple signal subtraction. The main advantage is the simplicity of the procedures that can be implemented in hardware for real time selective focusing. As an example in medical imaging, the detection of 3 reflectors located at 50 mm depth in tissues could last less than 10 milliseconds!.

This technique is also robust in speckle noise as it can be seen, for example, on a biological phantom containing 9 wires embedded in a random distribution of unresolved scatterers. Figure 13.a shows the beamformed pulse-echo image of the phantom when it is illuminated with a plane wave. We can see the echoes of some target superimposed to the speckle noise. The iterative method is able to identify easily the 9 echoes as it is shown in figure 13.b.

Compared to a conventional B scan image (figure 13.c), our technique is able to perfectly recognize the 9 targets. Using the time delays, the position of each target can be estimated and, in figure 13.d, the positions of the targets are superimposed to the basic image. An interesting application of this technique is the identification of micro calcifications in the breast or other organs.

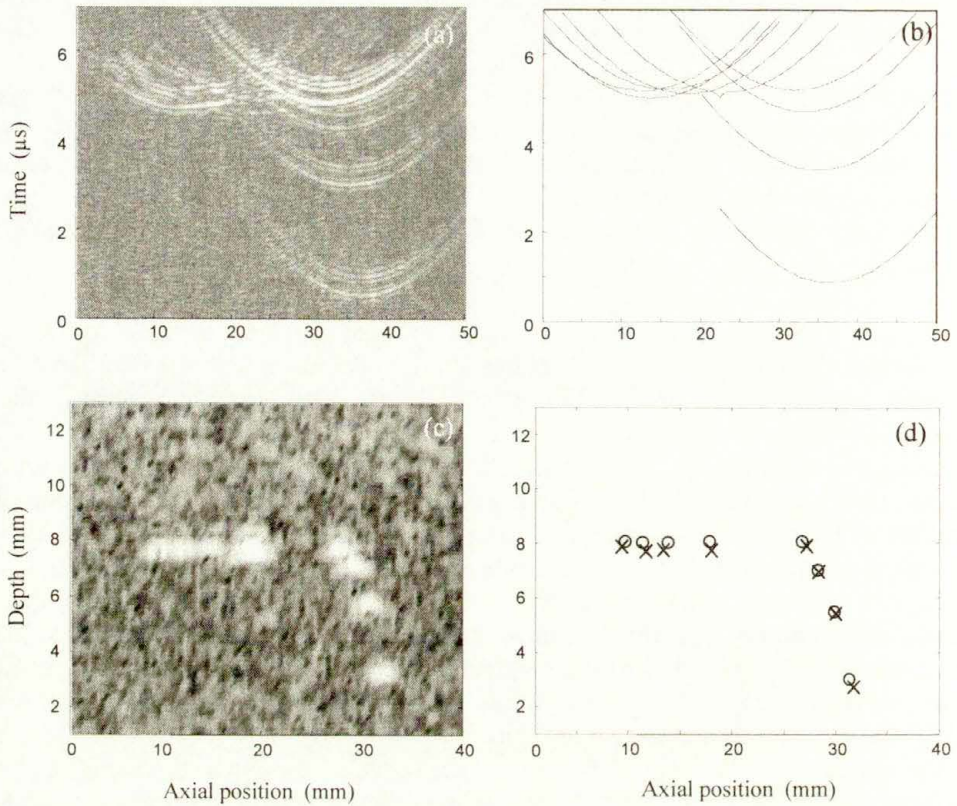


Fig. 13. Target detection in a biological phantom.

(a) Signals received after a plane wave illumination, we can see echoes of the targets embedded in an important speckle noise.

(b) Detection of the 9 target echoes.

(c) B-scan image of the phantom.

(d) Calculation of the targets positions from the detected echoes. Crosses correspond to the measured positions and circles correspond to positions given by the phantom furnisher.

### 3. Time reversal in dissipative media : Application to brain therapy

Another major promise of self-focusing TRM arrays is ultrasonic medical hyperthermia. In this technique, high intensity ultrasound produces thermal effects. A part of the ultrasound energy is absorbed by the tissue and converted to heat, resulting in an increase in local temperature. If local temperature rises above  $60^{\circ}\text{C}$ , tissue destruction can occur within seconds. Focused ultrasound surgery, pioneered in the 1950s by W. Fry at the University of Illinois [11,12,13], has not gained general acceptance until recently. Focal probes consisting of annular phased arrays are now marketed for the treatment of prostate cancer. These techniques are limited

to the production of necrosis in tissues that are not moving ; however, applications to abdominal and cardiac surgery are limited by the tissue motion induced both by the cardiac cycle and by breathing. At the University of Michigan, E. Ebbini and his group are developing self-focusing arrays to solve this problem [14,15,16]. In our group, we are working on TRM application for brain hyperthermia. The challenge of this application is to focus high-power ultrasound beams through the skull bone for local destruction of malignant brain tumors. Hynynen and his group have developed phased array techniques, without amplitude correction, to focus through the skull [17,18,19] However, the skull induces not only severe refraction and scattering of the ultrasonic beam [20], but also, the porosity of the skull bone produces a strong dissipation that breaks the TR symmetry of the wave equation. It has been shown [21,22] that TR focusing is no longer appropriate to compensate for the skull properties and a new focusing technique have been developed in our group that combines a correction of the dissipative effects with classical TR focusing. In a first step, this technique allows to focus on an artificial source implanted inside the treatment volume during the NMR guided biopsy. In a second step, the ultrasonic beam is steered on points surrounding this beacon in order to investigate and burn the whole volume of the tumor.

Experiments were first conducted with a 1D prefocused cylindrical array of transducers made of 128 piezoelectric elements working at a central frequency of 1.5 MHz ( $\lambda = 1$  mm). A dried human skull has been cut in the midsagittal plane and stored in a water tank and is located between the source and the array of transducers, its outer side is about 40 mm away from the skull (Fig. 14).

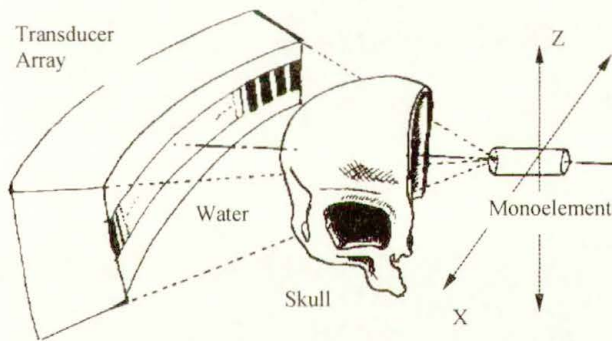


Fig. 14. Experimental set-up.

Figure 15 shows the directivity patterns of the focused beams in three different cases. First a reference pattern is obtained through water with cylindrical focusing (solid line). Introducing the skull induces a severe defocusing of the cylindrical beam (dashed line) : the beam is widely spread. However, the result obtained with TR focusing is also poor (dotted line). This figure shows that TR focusing is slightly better but remains far from the optimum. In order to understand this behavior, the

wavefront, coming from the source, and recorded by the 128 transducers is presented in gray scale on Fig. 16.

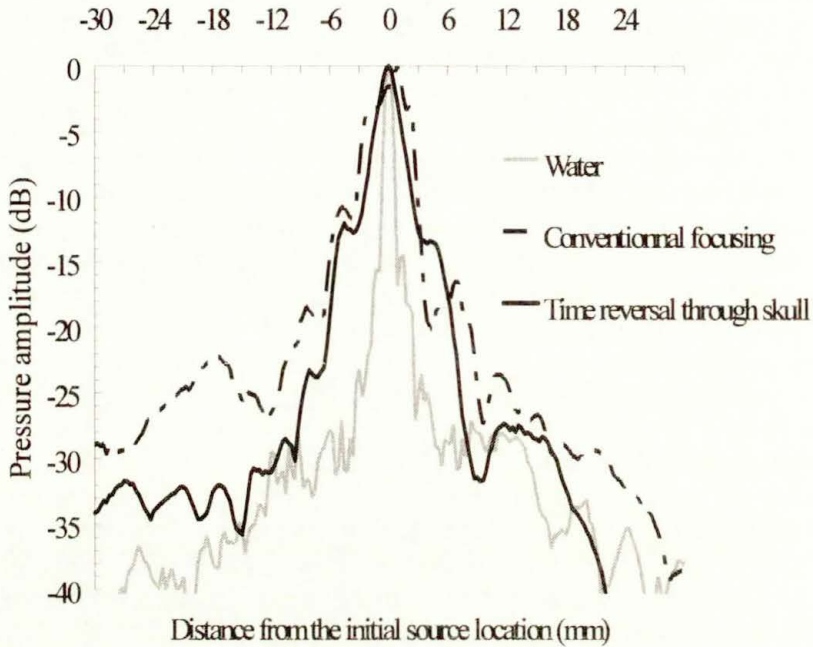


Fig. 15. Directivity patterns obtained by time reversal through pure water (grey line), focusing through the skull assuming a homogeneous medium (dotted line), time reversal through the skull (solid line).

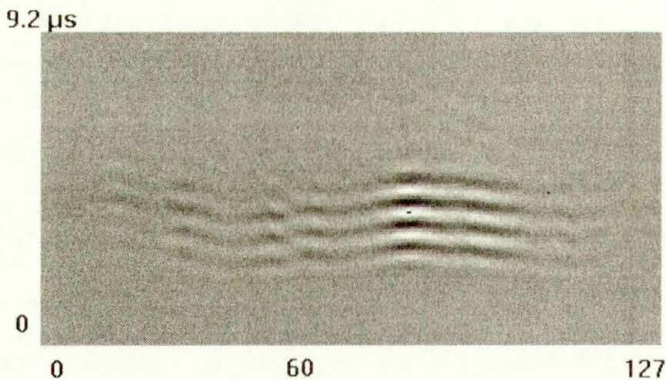


Fig. 16. Waveforms received through the skull.

We can observe not only a phase distortion of the wavefront, a strong amplitude modulation is also visible. In this experiment, the amplitude modulation is mainly due to absorption losses that occur in the skull and cannot be compensated by the time-reversal operation. Indeed, the transducer elements located in front of a strong absorbing region receive and transmit after the time-reversal operation a signal of small amplitude. Thus, when the wavefront goes back through the aberrating layer, the amplitude modulation is even squared.

From a mathematical point of view, the time-reversal focusing method is related to the invariance of the wave equation under the change of  $t$  to  $-t$ . However, acoustic losses are taken into account in the wave equation by a first-time derivative and are no more time-reversal invariant

In order to improve the TRM focusing, a first pretreatment that takes into account the amplitude modulation due to absorption can be added. If we assume that the skull can be modeled as a thin random absorbing phase screen located close to the array, the amplitude modulation is only due to absorption losses. The amplitude modulation is estimated by comparison with a reference waveform obtained in the same condition in a homogeneous medium. This estimation is used to invert the amplitude modulation of the wavefront. Figure 17 shows the wavefront after this amplitude compensation. Then, the compensated wavefront is time-reversed and transmitted.

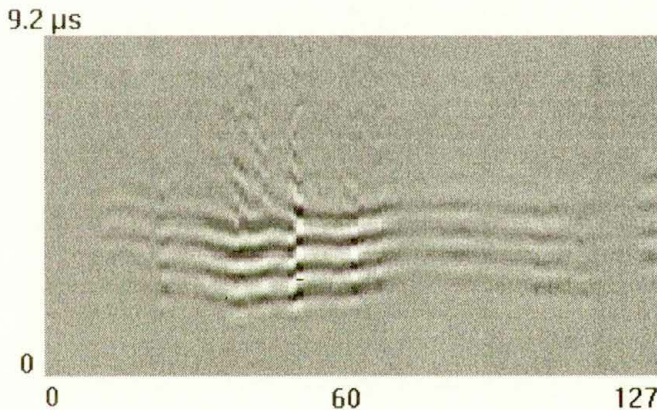


Fig. 17. Waveforms received through the skull after amplitude compensation.

The corresponding directivity pattern is plotted on Fig. 18 (dotted line). The amplitude compensation improves focusing, and the beamwidth is perfectly corrected up to  $-14$  dB below the peak. However, in real experiments, this compensation is not optimal. Indeed, due to mechanical and thermal problems, the array is located in the water tank at 40 mm from the skull. The wavefront, coming from the source, after passing through the skull, has to propagate towards the array on 40 mm water depth. During this step, new phase and amplitude modulations are added. They are automatically compensated by the backpropagation of the time-

reversed wavefield and so, must not be taken into account a second time in the pretreatment. To improve the focusing process, the amplitude compensation must be applied only to the amplitude distortion due to acoustic losses in the skull. For this purpose, amplitude distortion developed during propagation from the skull to the receiving aperture can be reduced by a numerical time-reversal operation. This numerical backpropagation of the received wavefront toward the aberrating layer is similar to the one presented by Fink and Dorme [23,24], and uses the Green's function of the homogeneous medium. Thus, the original diverging wavefront recorded by the array is first backpropagated numerically from a 100 mm to a 60 mm radius of curvature cylindrical surface, respectively corresponding to the array aperture and the skull surface. Amplitude distortion is then estimated along the skull surface. An amplitude compensated waveform is then computed on this surface and numerically backpropagated from the skull to the array. Thus, a new set of 128 signals matched to the initial source location are computed. These signals are time-reversed and experimentally transmitted in the medium. Figure 18 shows a comparison of the focusing results obtained with amplitude compensation in the aperture (dotted line) and amplitude compensation after backpropagation (dashed line).

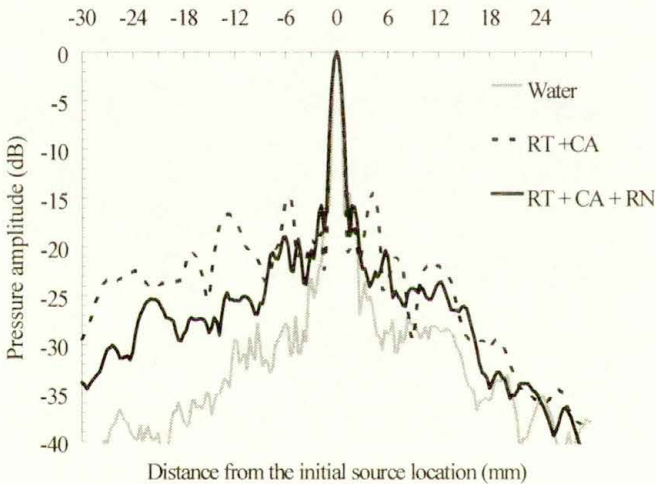


Fig. 18. Directivity patterns obtained by time reversal through pure water (grey line), time-reversal with amplitude compensation in the aperture (dotted line) and time-reversal with amplitude compensation after backpropagation (solid line).

The main improvement is on the side lobe level -12 dB below the main peak level. Note that in this study, a 1D array is used. Since significant aberration exists both in elevation and azimuth, aberration correction should be performed in both dimensions to be most effective. Nevertheless, this focusing quality seems quite good for hyperthermia, where the heating pattern contrast is proportional to the

ultrasound energy. In conclusion, we have shown that absorption can cause dramatic beam degradation. This experiment emphasizes the difference between time-reversal invariance and matched filter. Indeed, the spatial reciprocity theorem holds even in the case of an absorbing medium. Therefore according to the matched filter theory, each individual transducer contribution reaches its maximum at the same time  $T$  at the source location, allowing a constructive interference. But this theorem does not predict anything about the pressure obtained at other locations and times. An amplitude compensation combined with the time-reversal method is required to improve focusing

Although amplitude compensation and time-reversal allow self-focusing on an artificial source implanted inside the treatment volume, the beam has to be steered on points surrounding this beacon to treat a tumor. In homogeneous media, conventional beamsteering consists in tilting the wavefront focused on the artificial source. This can be obtained by delaying the pulses according to a tilted delay law. In heterogeneous media, this process is only valid for small angles or when aberrations are located close to the array. Indeed, this angle depends on the coherence length of the aberrating layer and on its position with respect to the array (this problem is equivalent to the determination of the isoplanetic angle in astronomy). Nevertheless, numerical backpropagation allows to extend this method to aberrating layers located at any distance from the array. The process is applied to focus at 5, 10 and 15 mm away from the initial source location. Figure 19 shows a comparison of the oblique directivity patterns obtained in three cases. The solid line shows the effect of tilting the wavefront in water only by delaying the signals with an oblique law. The dotted line shows, in presence of the skull, the effect of both tilting and amplitude compensation of the wavefront in the array aperture and the dashed line shows the result obtained by tilting and amplitude compensation of the wavefront after numerical backpropagation to the skull. Without backpropagation, the focusing is quickly degraded as the distance from the initial source location increases, thus sidelobes appear respectively at -12 dB, -6 dB and -2 dB. On the other hand, the focusing remains quite good when backpropagation to the skull-array distance is applied before amplitude compensation and tilting of the wavefront. Sidelobes appear respectively at -12 dB, -12 dB and -14 dB. Conventional beamsteering that consists in tilting the wavefront without backpropagation is no longer efficient when the aberrating and absorbing layer is located far away from the transducer array. These results clearly show the possibility of controlling the shape of an ultrasonic beam through the skull on a large region surrounding an artificial source.

All the preceding results were obtained with 1D array. Recently we have extended this technique to 2D array in order to obtain 3D focusing [25]. We have built a fully programmable random sparse 2D array for non invasive transskull brain therapy. The central frequency of the transducers has been set to 1MHz. In order to correct the phase and amplitude distortion induced by the skull, the active element size has to be smaller than the correlation length of the skull (approximately 1 cm at 1MHz). Moreover, the element size has to be small enough to permit beam steering in a sufficiently large volume. The array is made of 200 high power transducers

(Imasonic, Besançon, France) with a  $0.5 \text{ cm}^2$  active area, enabling us to obtain 300 bars at focus.

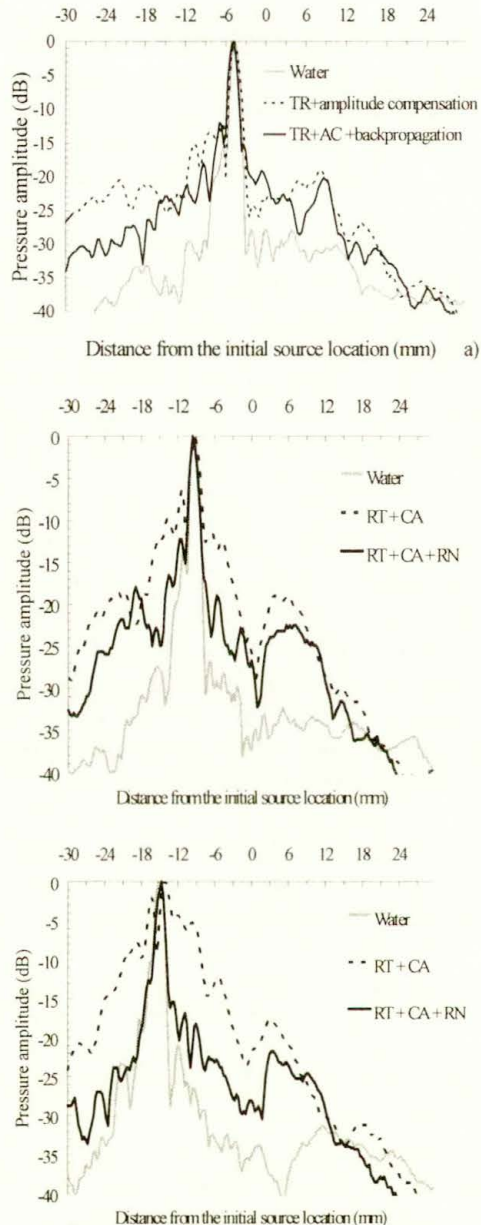


Fig. 19. Directivity patterns obtained by tilting the wavefront received from the initial point source at a distance of (a) 5 mm, (b) 10 mm and (c) 15 mm : Tilting through pure water (grey line), time-reversal of the signal received through the skull with amplitude compensation (dotted line), time-reversal of the amplitude compensated signal after backpropagation (solid line).

The time reversal process combined with amplitude compensation was performed at the geometric center of the array in order to correct for phase and amplitude aberrations induced by the bone on the ultrasonic beam. The resulting intensity field was scanned in the focal plane. It is shown in figure 20 and compared with the field obtained without any aberration corrections.

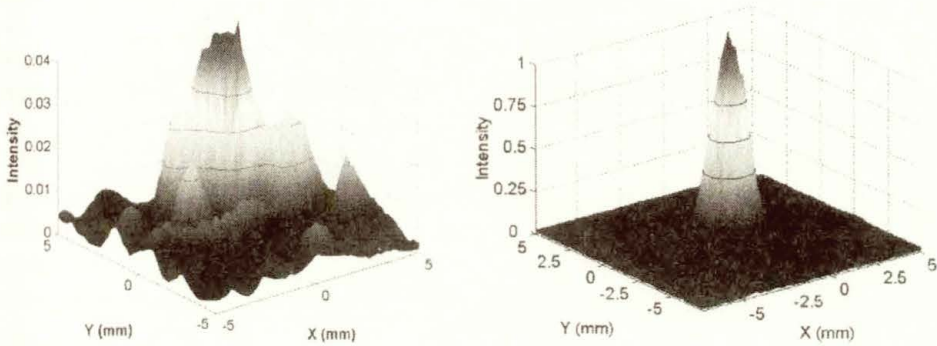


Fig. 20. Experimental distribution of the normalized intensity in the focal plane  
 (a) Without aberrations corrections  
 (b) With corrections. Black lines correspond to -3 dB, -6 dB and -9 dB.

The uncorrected beam is strongly degraded by the skull. The focal spot is not at the desired location and is widely spread in comparison with the corrected one. Moreover, an important point is that the pressure amplitude at focus of the corrected beam (70 Bars) is 4.5 times higher than the pressure amplitude of the uncorrected one. Consequently, it results in a 22 times higher heat deposit. In order to check experimentally the heating pattern and the steering capabilities obtained through the skull a plexiglas slice (10 mm width) was placed behind the skull so that its first interface is located in the focal plane of the system. A 2 seconds insonification was achieved and induced a burning at the plexiglas interface. The emission signals were then tilted electronically in order to focus at several locations in the four cardinal directions. As one can notice in figure 21a, the targets are clearly defined, the "plexiglas necrosis" size is about 1.5 mm diameter. The impact is more important at the geometrical center of the system as the focal pressure amplitude decreases when tilting the beam. The same kind of experiments were conducted, behind the skull in fresh liver samples and very precise necrosis were obtained (Fig 21 b). Two 5 seconds sonifications were performed at each location. The high precision electronic beam steering allows to induce very precise necrosis whose shape could be adapted to each target. As an example, a square-shaped necrosis was performed with 25 shots with a 2mm spatial pitch. Further works will be soon investigated in vivo on 20 sheeps.

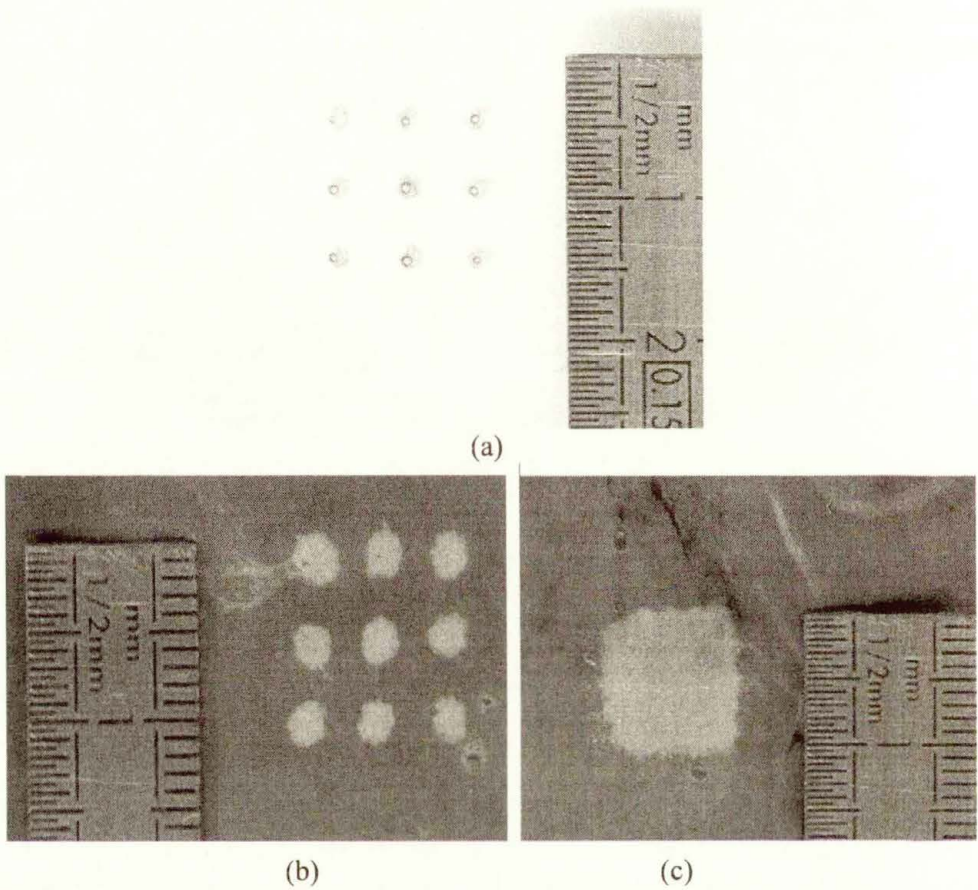


Fig. 21.

(a) Impacts induced in a slice of plexiglas located in the focal plane ( $Z = 120$  mm) through the skull. The impact size is about 2 mm. Aberration corrections were achieved at center by using an hydrophone and next impacts were achieved by tilting electronically the beam.

(b,c) Lesions induced in fresh liver through a human skull. The target is located at depth  $Z = 120$  mm from the array. In both experiments the aberration corrections were achieved at center by using an implanted hydrophone and the other impacts were achieved by tilting electronically the beam. b) Lesion size is about 2 mm in diameter for the center spot. The spatial pitch between each lesion is 5 mm. c) Square-shaped necrosis performed with 25 focus (2mm spatial pitch).

#### 4. Time reversal in waveguides : compact shock wave generator

Here we show that time reversal techniques allow not only to adaptively focused a wave through aberrating media but also to revisit the concept of piezoelectric transducer design. Time reversal focusing can also be developed in reverberating media such as cavities or waveguides. Contrary to conventional transducer technology avoiding unwanted reverberations in piezoelectric elements, time reversal can take benefit of strongly reverberating media to increase the transducer efficiency. We will demonstrate that very high pressure fields can be obtained with a small number of transducers connected to reverberating media such as solid waveguides. It leads to a new generation of ultra-compact shock wave lithotripters.

We have seen in 1.2 that the use of piezoelectric transducer arrays has opened up the possibility of electronic steering and focusing of acoustic beams to track kidney stones. However, owing to the limited pressure delivered by each transducer (typically 10 bar), the number of transducers needed to reach an amplitude at the focus on the order of 1000 bars is typically of some hundreds of elements, that makes a very expensive device. The idea is to take advantage of the temporal dispersion in the waveguide to create, after time reversal, a temporally recompressed pulse with a stronger amplitude.

Time reversal focusing has been previously studied in waveguides in the field of ultrasound [26,27] and in ocean acoustics[28,29,30]. A simple experiment conducted by P. Roux et al in an ultrasonic wave guide shows the effectiveness of the TR processing not only to focus but also to compensate for the temporal dispersion of a waveguide. A point-like source is located in a water channel bounded by two plane and parallel interfaces (a water/air interface and a steel/water interface). A 96 elements TR array is located, in the waveguide, at 800 mm from the source. Fig. 22a and 22b shows the transmitted field recorded by the array after the propagation through the channel. After a first wavefront corresponding to the direct path, a set of signals corresponding to the multiple reflexions of the incident wave on the interfaces is observed. Figure 22c shows the wavefield measured at the source location after time-reversal of the first 100  $\mu\text{s}$  of the received signal (ten first arrivals). The time reversal operation compensates multipath effects and an impressive time recompression is observed.

The TR beam is focused on a spot which is much thinner than the one observed in free water. This can be interpreted by the theory of images in a medium bounded by two mirrors. For an observer, located at the source point, the 40 mm high TRM seems to be escorted by an infinite set of virtual images related to multipath propagation. Thus, taking into account the 10 first arrivals, the effective aperture of the TRM is nearly 10 times larger than the real aperture. This very interesting property of time reversal in waveguides can be used to increase the effective size of the array.

Another advantage of time reversal in multiple scattering or reverberating media is the extreme robustness of TRM. Compared to classical time reversal mirrors that usually work with 8 bits A/D resolution, we have shown that 1 bit time reversal operations provide the same temporal and spatial focusing results [31].

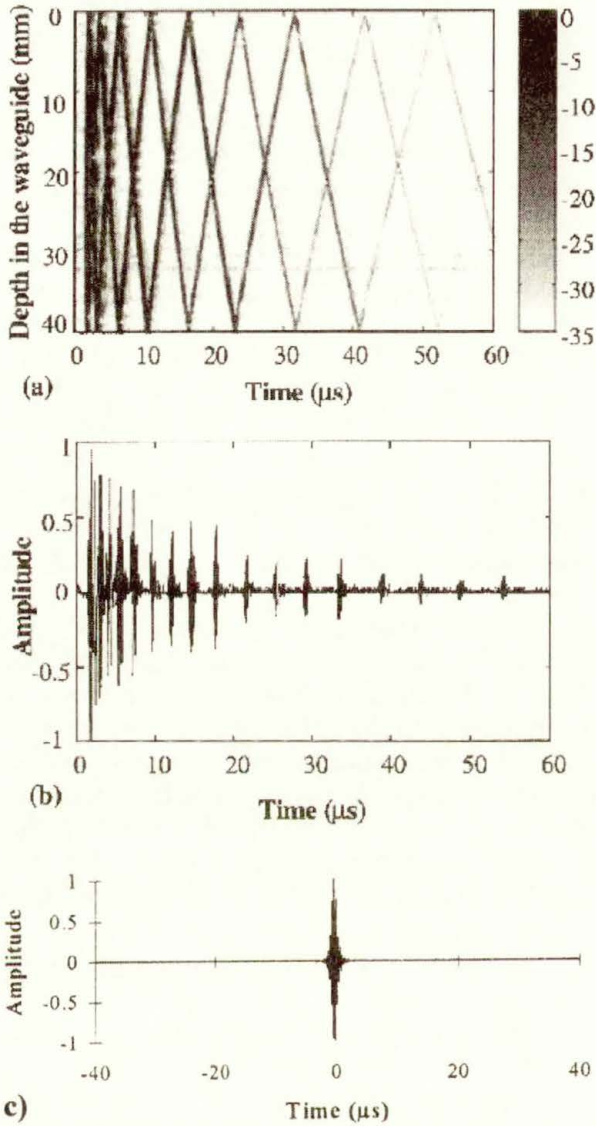


Fig. 22.

(a) The wavefront transmitted by a point like transducer through the wave guide. The wave front is recorded by the 96 element array. Note that after the direct wave, the reverberation in the waveguide gives rise to a set of 10 multiply reflected wavefronts.

(b) The wavefront recorded by an individual transducer. Most of the wave energy is located in the multipaths.

(c) The time-reversed wave measured at the initial source position. Multipath effects are completely compensated and an important time compression is observed.

In Fig. 23, a schematic of the complete experimental setup puts in evidence the characteristics of the system [32,33]. Time reversal is performed between a point source (in S) in water and seven 8-mm-diameter piezoelectric transducers attached to a section of a 3.2-cm-diam (in A), 50-cm-long duraluminium cylinder.

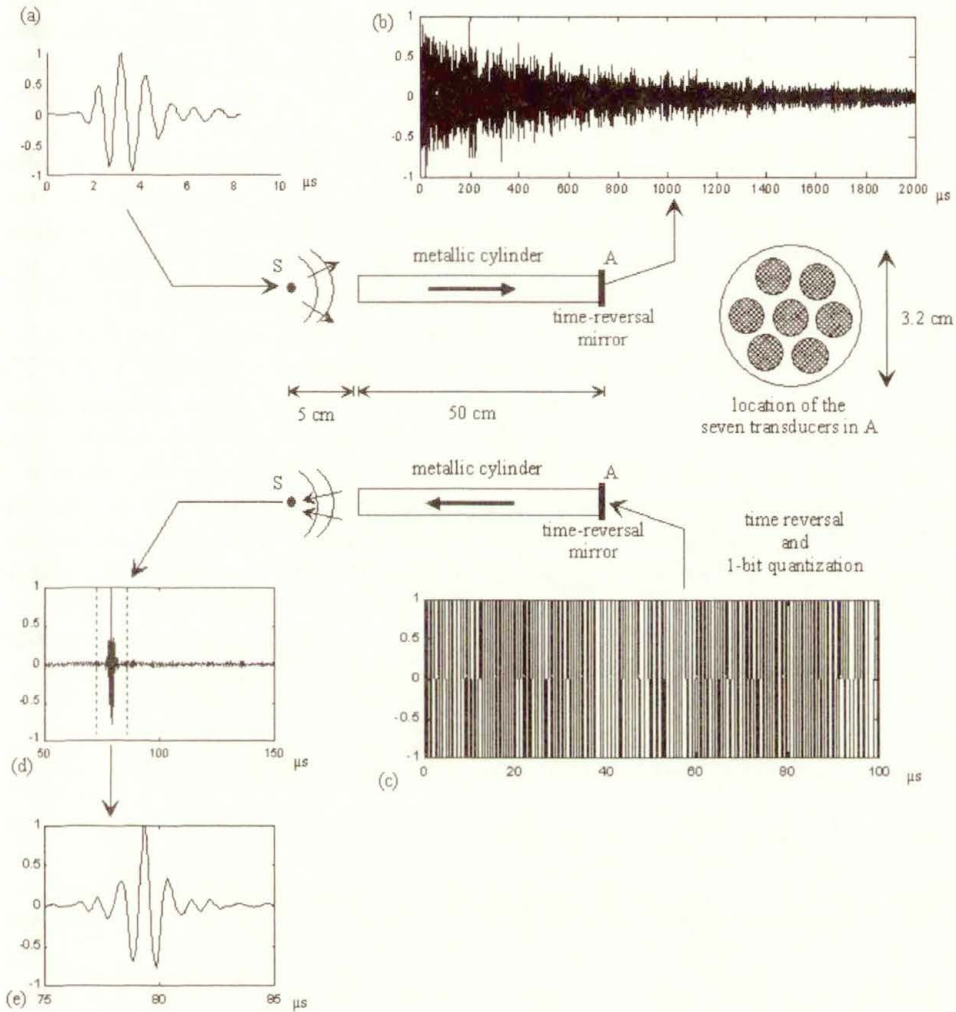


Fig. 23. Experimental demonstration of 1-bit time reversal in a waveguide : (a) the acoustic source transmits a pulsed signal in water; (b) normalized signal received on one of the seven transducers in A at the end of the 50-cm long, 3.2-cm diameter metallic waveguide; the signal spreads over more than 2 ms; (c) the signal is time reversed, 1-bit numerized and retransmitted from the same transducer in A. For presentation reason, only the first 100  $\mu\text{s}$  are plotted; (d) normalized signal obtained in S after 1-bit time reversal from the seven transducers in A and back propagation through the guide; (e) zoom of the time reversed signal between the dashed lines : the time-reversed signal (e) is similar to the source signal (a).

The central frequency is 1 MHz with a 75% band-width, which corresponds to a 5-mm central wavelength for compressional wave in duraluminium. The bottom end of the metallic cylinder is immersed in water at a distance  $d$  from the source ( $d$  between 0 and 10 cm). Each transducer is connected to an electronic circuitry which consists of two 8-bit D/A and A/D converters having a 15-MHz sampling rate, to receive the incident signal and transmit the time-reversed signal; Classical time reversal is then 8-bit time reversal. On the other hand, during a 1-bit time reversal experiment, only the sign of the time-reversed signal is transmitted ( $+V$  if  $s(t) > 0$ ,  $-V$  if  $s(t) < 0$ , where  $V$  is the maximum amplitude of the input signal).

Figure 23 b represents the signal received on one transducer in A after transmission of a pulse from the source in S. As expected, the signal spreads in time because of many reverberations on the interfaces of the solid wave-guide. The signal lasts more than 2000  $\mu\text{s}$ , i.e., around 1000 times the length of the initial pulse. In a duraluminium sample, 2 ms corresponds approximately for a longitudinal wave to a 10-m distance, to be compared to the 50-cm length of our cylinder. This means that many round trips inside the cylinder are present in the dispersed signal. In Fig. 23c we show a 100- $\mu\text{s}$  window of the 1-bit time-reversed version of the incident signal. Figure 23d corresponds to the signal obtained at the source in water after back propagation through the solid guide with 1-bit time reversal. We observe a remarkable time compression on the initial source in S. This confirms that the instantaneous amplitude information which has been ignored with 1-bit time reversal is not necessary to successfully perform a time reversal experiment in a solid waveguide.

In Fig. 24, we compare the time reversed signal at the source with 1-bit and 8-bit time reversal respectively.

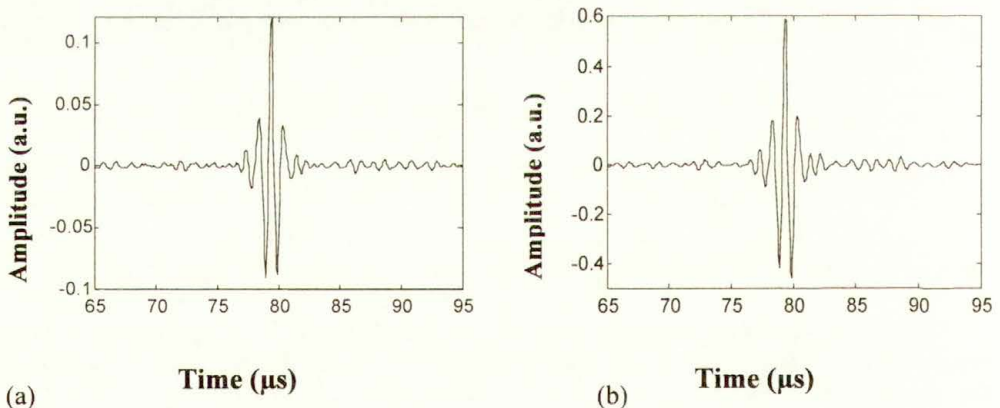


Fig. 24. Comparison between (a) 8-bit time-reversal and (b) 1-bit time-reversal. Time reversal is performed by seven transducers fastened at one end of the guide (in A). The source is placed in water at 6 cm from the other end of the guide.

The major difference between 1-bit and 8-bit time reversal lies in the amplitude of the signal received in S : the instantaneous power obtained with 1-bit time reversal is 4 times higher than the instantaneous power obtained with 8-bit time reversal, which is itself higher than the power transmitted into the water by the transducer without waveguide. The amplification obtained between 1-bit and 8-bit time reversal can be easily understood by comparing Figs. 23b and 23c : indeed, more energy has been delivered into the waveguide (and then to the source) with 1-bit time reversal because the natural decrease of the signal has been compensated. What happens now at the source? For a linear system characterized by its impulsional response  $h(t)$ , the response  $R(t)$  at an excitation  $f(t)$  is:

$$R(t) = h(t) \otimes f(t) \quad (1)$$

Time reversal uses as excitation the time reversed version of the impulsional response, which implies :

$$R(t) = h(t) \otimes h(-t) \quad (2)$$

It is well known that  $R(t)$  is then symmetrical with a maximum at  $t=0$ . Let us find out now what is the input signal  $f(t)$  - defined such as  $|f(t)| \leq 1$  - that produces the maximum output amplitude at  $t=0$ . Writing Eq. 1 as an integral, we get :

$$R(0) = \int f(\tau)h(-\tau)d\tau \leq \int |f(\tau)||h(-\tau)|d\tau \quad (3)$$

As we suppose  $|f(t)| \leq 1$ , it follows :

$$R(0) \leq \int |h(-\tau)|d\tau = \int \text{sign}(h(-\tau))h(-\tau)d\tau \quad (4)$$

Thus :

$$R(0) \leq \text{sign}(h(-t)) \otimes h(-t) \Big|_{t=0} \quad (5)$$

This implies that the maximum amplitude of the output of a linear system is obtained using as input the sign of the time-reversed impulsional response of the system. Thus 1-bit time-reversal delivers at the source a higher maximum amplitude than 8-bit time-reversal.

A comparison between the performances of this time reversal prototype and a reference transducer of diameter 32 mm has been made and the final pressure amplitude that is achieved experimentally is 15 times larger. As an example, we used an applied tension of +/- 170 V applied on each of the seven transducers in order to produce shock waves on a piece of chalk. With this prototype, the estimated pressure at the focus is 500 bars [32,33]. Figure 25 shows how different perforations are obtained on the chalk with 150 to 600 impacts.

We are now testing a new generation of lithotripter that consist of a larger 10-cm diameter cylinder with 32 transducers. It would reach more than 2000 bars at the focus. In view of application to lithotripsy, such a device would combine several advantages. Firstly, the cylinder diameter would be small compared to classical 30-cm diameter lithotripters. Secondly, the transducers would be excited at a low voltage and would not be directly submitted to the high-power shock waves and therefore the lifetime of the system would be increased. Finally, its price, in relation

to the number of independent one-bit electronics, will be greatly reduced compared to a classical lithotripter made of more than 100 transducers.

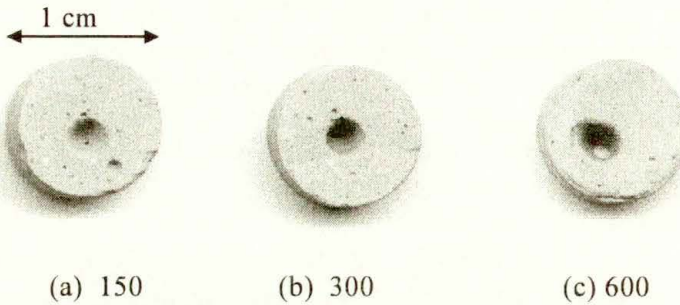


Fig. 25. Perforation observed in pieces of chalk with  $\pm 170$  V excitation. (a) 150 shots, (b) 300 shots, (c) 600 shots.

## 5. Conclusion

Time-reversal shows startling applications in the field of acoustics. Because acoustic time-reversal technology is now easily accessible to modern electronic technology, it is expected that applications in various areas will rapidly expand. Initial applications show promise in medical therapy. We have shown in this paper how passive reflecting targets embedded in the body (kidney stones, breast microcalcifications....) can be used as sources of time reversal waves. The very first and perhaps most illustrative application of time reversal concerns real time tracking and destruction of moving kidney stones during lithotripsy treatment. Iterating the time reversal process leads also to interesting applications as it becomes possible in multiple targets environments to select and focus in real time on each target of a medium. For this purpose, the ability of iterative time reversal to improve the detection of microcalcifications in the speckle noise of the breast was presented.

Time reversal is also a very powerful correction technique for distortions induced by sound velocity and density heterogeneities. Combined with absorption correction techniques, its potential is currently investigated for the local destruction of malignant brain tumors using trans-skull high intensity focused ultrasound.

Beyond these straightforward applications of time reversal to spatial focusing of waves through aberrating medium, time reversal techniques allow also to revisit the complete concept of piezoelectric transducer designing. Contrary to conventional transducer technology avoiding unwanted reverberations in piezoelectric elements, time reversal can take benefit of strongly reverberating media to create virtual transducers and thus to obtain a very high focusing quality with a small number of transducers. We have shown how it should lead to a new generation of ultra-compact shock wave lithotripters. The application of this breakthrough concept for 3D medical imaging is also currently investigated.

All these applications of time reversal were discussed in the field of linear acoustics, but a very interesting point is that time reversal properties remain valid in the field of nonlinear acoustics. We are currently envisioning that time reversal techniques can also be very useful in nonlinear acoustics as it could enhance the image contrast in medical harmonic imaging.

## References

- [1] M. Fink, "Time Reversal of Ultrasonic Fields : Basic Principles", IEEE Trans. Ultrason. Ferroelec. Freq. Contr, 39 (5) 555-566 (1992)
- [2] C. Prada, F.Wu, M.Fink, "The Iterative Time Reversal Mirror : A solution to self focusing in pulse-echo mode", J.Acoust.Soc.Am, 90 (2), 1119-1129 (1991).
- [3] JM. Delius "Lithotripsy," Ultrasound Med. Biol. 26, Suppl. 1, S55-S58 (2000).
- [4] S. Nachef, D. Cathignol, and A. Birer, "Piezoelectric electronically focused shock wave generator," J. Acoust. Soc. Am. 92, 2292 (1992).
- [5] J.L Thomas, F. Wu, M. Fink, "Time Reversal Mirror Applied to Litotripsy" , Ultrasonic Imaging, 18, 106-121, (1996)
- [6] C. Prada, M.Fink, "Eigenmodes of the time reversal operator : a solution to selective focusing in multiple target media ", Wave Motion, 20, 151-163 (1994).
- [7] C. Prada, J.L. Thomas, M. Fink, The iterative time reversal process : analysis of the convergence, J.Acoust.Soc.Am, Vol 97(1), 62-71, (1995).
- [8] C. Prada, S.Manneville, D. Spoliansly,M. Fink, "Decomposition fo the time reversal operator: Detection and focusing on two scatterers" J.Acoust.Soc.Am.,99, 2067-2076(1996).
- [9] D. H. Chambers and A. K. Gautesen. "Time reversal for a single spherical scatterer". J. Acoust. Soc. Am., 109 (6), 2616-2624, 2001.
- [10] G.Montaldo, M.Tanter, M. Fink,"Revisiting iterative time reversal process : applications to ultrafast multiple target detection"submitted to J. Acoust. Soc. Am, Nov. 2002.
- [11] W. J. Fry, J. W. Barnard, F. J. Fry, R. F. Krumins, and J. F.Brennan, "Ultrasonic lesions in the mammalian central nervous system," Science, vol. 122, pp. 517-518, (1955).
- [12] J. Driller and F. L. Lizzi, "Therapeutic applications of ultrasound: A review," IEEE EMB Magazine, vol. 6, no. 4, 33-40,(1987).
- [13] F. Kremkau, "Cancer therapy with ultrasound: A historical review," J. Clin. Ultrasound, vol. 7, pp. 287-300, (1979).
- [14] E. S. Ebbini and C. A. Cain, "Multiple-focus ultrasound phased-array pattern synthesis: Optimal driving-signal distributions for hyperthermia," IEEE Trans. Ultrason., Ferroelect., Freq.Contr., vol. 36, 540-548, (1989).

- [15] E. S. Ebbini, Deep localized hyperthermia with ultrasound phased arrays using the pseudoinverse pattern synthesis method," *IEEE Trans. Biomed. Eng.*, vol. 38, pp. 634-643, 1991.
- [16] H. Wang, E. S. Ebbini, M. O'Donnell, and C. A. Cain "Phase aberration correction and motion compensation for ultrasonic hyperthermia phased arrays: Experimental results," *IEEE Trans. Ultrason., Ferroelect., Freq. Contr.*, vol. 41, 34-43, (1994).
- [17] J. Sun, K. Hynynen, "Focusing of therapeutic ultrasound through a human skull: A numerical study", *J. Acoust. Soc. Am.*, vol. 104(3), pp.1705-1715 (1998).
- [18] J. Sun and K. Hynynen, 'The potential of transskull ultrasound therapy and surgery using the maximum available surface area', *J. Acoust. Soc. Am.*, vol. 105, pp.2519-2527 (1999).
- [19] G. T. Clement, J. P. White and K. Hynynen, 'Investigation of a large area phased array for focused ultrasound surgery through the skull', *Phys. Med. Biol.*, vol. 45, pp.1071-1083 (2000).
- [20] F. Fry and J. Barger, "Acoustical properties of the human skull", *J. Acoust. Soc. Am.*, 63(5), 1978, pp. 1576-1590.
- [21] J.-L. Thomas, M. Fink, "Ultrasonic beam focusing through tissue inhomogeneities with a time reversal mirror: application to transskull therapy", *IEEE Trans. Ultrason., Ferroelect., Freq. Contr.*, vol. 43, no. 6, 1122-1129, (1996).
- [22] M. Tanter, J.-L. Thomas and M. Fink "Focusing and steering through absorbing and aberrating layers: Application to ultrasonic propagation through the skull" *J. Acoust. Soc. Am.*, Vol. 103(5) pp. 2403-2410 (1998).
- [23] C. Dorme, M. Fink, " Focusing in transmit-receive mode through inhomogeneous media : the time reversal matched filter approach", *J. Acoust. Soc. Am.*, vol 98 (2), p 1155-1162, (1995).
- [24] M. Fink, C. Dorme, « Steering and focusing through inhomogeneous media with matched filter » *IEEE Trans. Ultrason. Ferroelec. Freq. Contr.*, vol 43 (1), p 167-175, (1996)
- [25] M. Pernot, J.-F. Aubry, M. Tanter, C. Dorme, M. Fink. " 200 elements fully programmable sparse array for brain therapy : simulations and first ex vivo experiments". *Proceedings of 2nd Intl. Symp. on Therapeutic Ultrasound*, Seattle, Ed Larry Crum( 2002).
- [26] P. Roux, B. Roman, M. Fink, « Time reversal in ultrasonic waveguide », *Appl. Phys. Lett* 70, 1811-1813 (1997).
- [27] P. Roux and M. Fink, "Time reversal in a waveguide : study of the temporal and spatial focusing", *J. Acoust. Soc. Am.*, 107 (5), pp 2418-2429, (2000).

- [28] W.A. Kuperman, W.S. Hodgkiss, H.C. Song, T. Akal, C. Ferla and D.R. Jackson, "Phase conjugation in the ocean : experimental demonstration of an acoustic time-reversal mirror", *J. Acoust. Soc. Am.*, 103(1), 25-40, (1998).
- [29] W.S. Hodgkiss, H.C. Song, W.A. Kuperman, T. Akal, C. Ferla and D.R. Jackson, "A long-range and variable focus phase conjugation experiment in shallow water", *J. Acoust. Soc. Am.*, 105(3), 1597-1604, (1998).
- [30] H.C. Song, W.A. Kuperman and W.S. Hodgkiss, "A time-reversal mirror with variable range focusing", *J. Acoust. Soc. Am.*, 103 (6), 3234-3240, (1998).
- [31] A. Derode, A. Tourin and M. Fink, "Ultrasonic pulse compression with one-bit time reversal through multiple scattering", *J. Appl. Phys.*, 85 (9), 6343-6352, 1999.
- [32] G. Montaldo, P. Roux, A. Derode, C. Negreira, M. Fink, "Generation of very high pressure pulse with 1 bit time-reversal in solid waveguides : applications to lithotripsy", *J. Acoust. Soc. Am.*, 110 (6) 2849-2857 (2001)
- [33] G. Montaldo, P. Roux, A. Derode, C. Negreira, M. Fink, "Ultrasound shock wave generator with one-bit time reversal in a dispersive medium, application to lithotripsy" *Appl. Phys. Lett.*, 80(5), 897-899 (2002)